Dynamics of Dissociative Recombination of Molecular Ions: Three-Body Breakup of Triatomic Di-Hydrides†

Sheldon Datz

Physics Division, Oak Ridge National Laboratory, P.O. Box 2008, Oak Ridge, Tennessee 37831-6377

Received: September 25, 2000

An electron, recombining with a molecular ion, deposits the negative of the ionization potential into the system and leads to dissociation into atomic and/or molecular fragments (dissociative recombination (DR)). Recent studies using heavy-ion storage rings have done much to elucidate the process. Relative collision energies as low as ∼1 meV are obtained, and information has been gained on total cross sections (rates), fragment branching fractions, and atomic states in DR of diatomic molecules. Tri-atomic di-hydrides (H_3^+, CH_2^+, NH_2^+, OH_2^+) show a propensity for dissociation into three fragments. To study the dynamics of this process, a new method has been used to obtain atomic excitation levels, distribution of energy, and angular distribution of the fragments. The case study of H_2O^+ has been completed and is discussed.

Introduction

Dissociative recombination (DR) is a process in which a free electron recombines with a molecular ion. The amount of internal energy given to the molecule in recombination is essentially the inverse of the ionization potential (e.g., IP ∼ 10−20 eV) and, as a result, the molecule dissociates, i.e.,

$$AB^+ + e \rightarrow AB^*(E = -IP) \rightarrow A + B + \Delta E \qquad (1)$$

The total exothermicity appears as a sum of internal-fragment excitation and recoil-kinetic energies. The DR process is of great consequence in determining the composition of low-temperature plasmas, e.g., cold interstellar clouds, planetary ionospheres, and edge plasmas in magnetic fusion devices. This process was first suggested by Bates and Massey in 1974.[1] The principal mechanisms envisioned for DR are demonstrated in Figure 1. The "direct" mechanism occurs when the collision energy is high enough to promote a vertical transition to a repulsive state of the neutral molecule. At lower energies (i.e., down to zero kinetic energy), one can have a resonant transfer to a Rydberg state of the neutral molecule followed by pre-dissociation.

Until approximately 1992, the experimental methods used, e.g., "flowing afterglow" were in most cases indirect. The final results generally involved assumptions about correlation processes and reactions. An additional and important difficulty being that molecular ions extracted from ion sources are generally in excited vibrational states, and it has been shown that DR is extremely sensitive to vibrational energy states. A more direct "single pass" merged beam method suffers from low-signal rates, and from the uncertainty of molecular ion internal energy states.[2] The advent of "cooled" ion storage rings opened new possibilities. The first suggestion that the rings could be used in DR studies was in 1992,[3] and the intensive studies in the last eight years have done much to elucidate this process.[4]

2. Ion Storage Rings

Ion storage rings that have been used to study atomic and molecular processes exist in Stockholm, Sweden; Aarhus, Denmark; Heidelberg and Darmstadt, Germany; and Tokyo, Japan. The Stockholm storage ring (CRYRING) is pictured in Figure 2. The extracted ions are first accelerated in the radio frequency quadrupole (RFQ) and injected into the ring where they are further accelerated and bent around the ring, contained by a set of dipole magnets. The maximum energy attainable varies with the individual ring. (In the case of CRYRING, the maximum energy is 96 q^2/M (MeV)) where q is the ionic charge and M is its mass.) During each revolution, the ion beam passes through a merged electron beam that is velocity matched to the ion beam. The primary function of the merged electron beam is to "cool" the translational momentum distribution of the ions by Coulomb scattering of the "hot" ion beam onto a continuously refurbished "cold" electron beam. For our purposes, this electron beam can also serve as a target for the recombination. Relative collision energies as low as ∼0.001 eV (∼10°K, ∼8 cm^{-1}) can be attained by merging with multi-MeV stored beams.

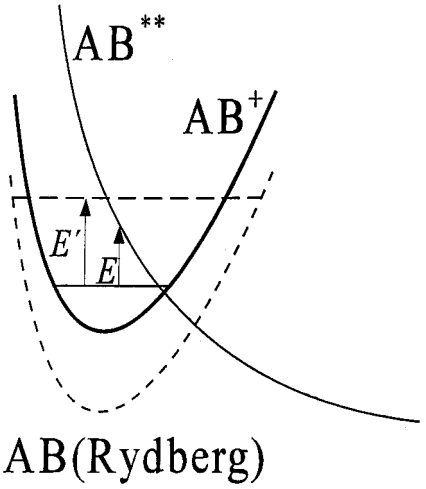

Figure 1. Dissociative Recombination. Two paths are shown. E, direct excitation of the AB^+ to a repulsive state of the neutral molecule; E′ electron capture to a Rydberg state of the neutral molecule.

For DR experiments, the molecular ion is injected into the ring and allowed to "float" for some seconds during which time, given a reasonable dipole moment, it can radiate down to its

† Part of the special issue "Aron Kuppermann Festschrift".

10.1021/jp003466c CCC: $20.00
Published on Web 02/07/2001

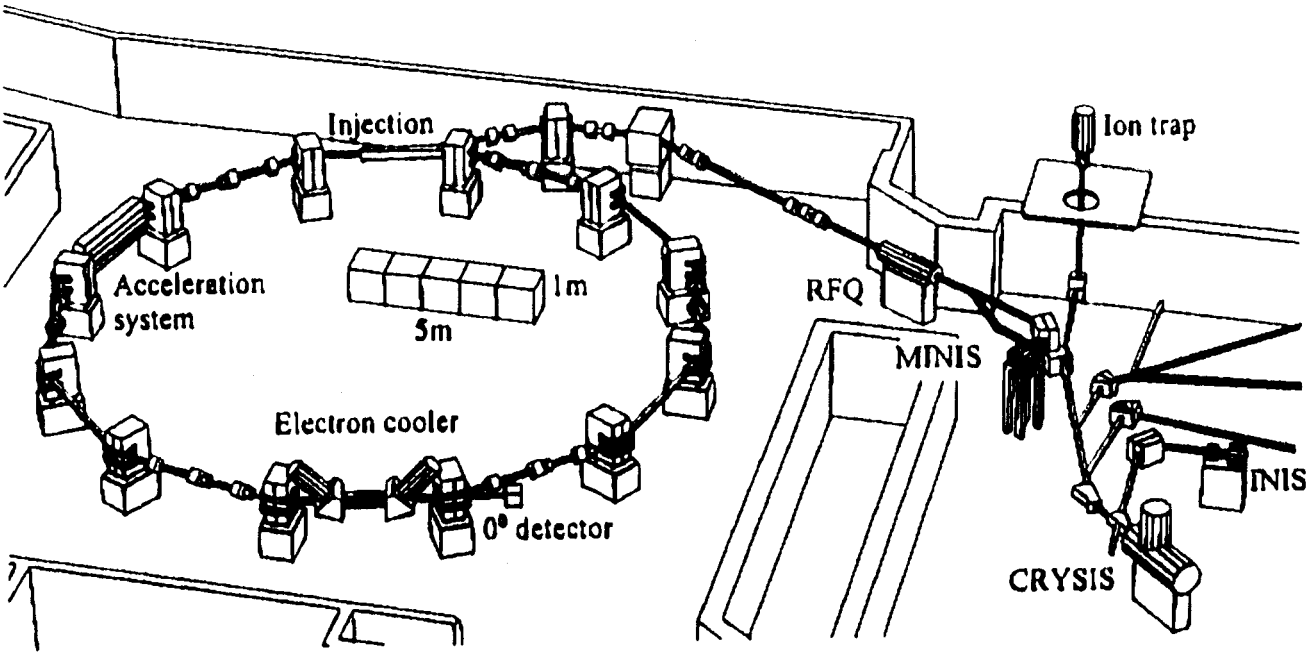

Figure 2. The CRYRING facility at the Manne Seigbahn Laboratory in Stockholm. Molecular ions are injected from the "MINIS," accelerated, and pass through the "electron cooler" which also acts as a merged electron beam target. Neutral fragments from DR exit at the O° detector.

vibrational ground state. DR takes place in the merged beam region, and the neutral fragments follow a straight path through the next dipole-bending magnet and strike a detector. The detectors used fall into two categories: (1) solid-state surface-barrier detectors which yield pulses heights proportional to the total energy deposited, and (2) position-sensitive, microchannel plate systems which are insensitive to the nature of the particle causing the pulse, but which can give high-resolution information on the positions of fragments striking the detector.

3. Total Cross Sections and Fragmentation

To illustrate this aspect of the work, I chose DR in H_3^+ [ref 5] and H_2D^+ [ref 6], i.e.,

$$H_3^+ + e \rightarrow H_3^* \quad (2a)$$

$$\rightarrow H_2 + H \quad (2b)$$

$$\rightarrow H + H + H \quad (2c)$$

$$H_2D^+ + e \rightarrow H_2D^* \quad (3a)$$

$$\rightarrow HD + H \quad (3b)$$

$$\rightarrow H_2 + D \quad (3c)$$

$$\rightarrow H + H + D \quad (3d)$$

mainly, because the right side of these equations look very much like the ones that have been of concern to Aron Kuppermann for much of his career. Total cross sections for DR of H_3^+ have been measured over 5 orders of magnitude in collision energy. These data was obtained using a solid-state surface-barrier detector. The beam was stored at ~5 MeV/amu. DR is signaled by the simultaneous arrival of three neutral particles; hence a pulse height on a solid-state surface-barrier detector corresponding to 15 MeV.

The fractions going into each channel (cf., e.g., 2a, 2b, 2c) were obtained by placing a "grid" in front of the detector (Figure 3).[6] The grid was 50-μm-thick steel and could be penetrated by the 5-MeV H atoms. The grid transparency was 31%. Particles passing through the holes gave full pulse height while those penetrating through the solid portion gave an attenuated pulse height (illustrated in Figure 4). Calculating the probability of a given pulse height for aggregates of one, two, and three particles gives the fraction breaking up into two or three fragments. Here came the first surprises. At low energies (~0 → 1 eV), three-particle breakup is dominant, i.e., the observed breakup fractions for H_3^+ were H_3^* (0%), H + H_2 (20%), and H + H + H (80%).[5] For H_2D^+ these fractions were $H_2D°$ (0%), HD + H (13%), H_2 + D (7%), and H + H + D (80%).[6]

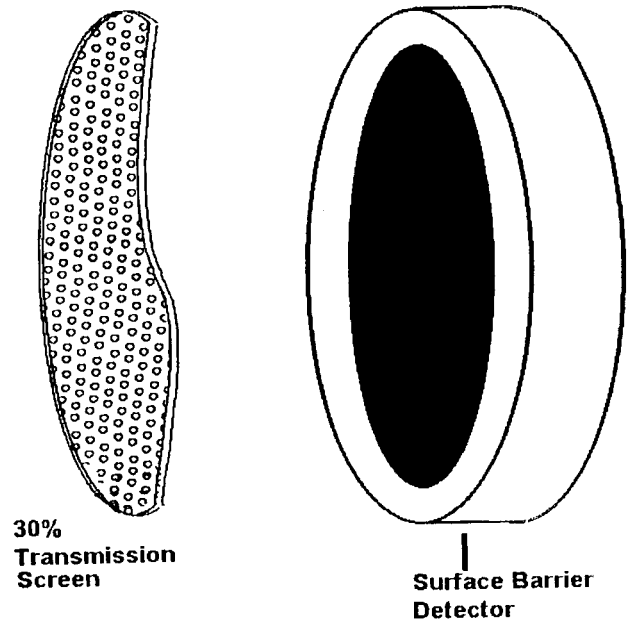

Figure 3. Detector system used for measurement of fragmentation pattern of H_3^+, H atoms passing through the holes yield a full-energy pulse of 6.5 MeV. H atoms at this energy can pass through the solid but yield a pulse of 4.7 MeV (see Figure 4).

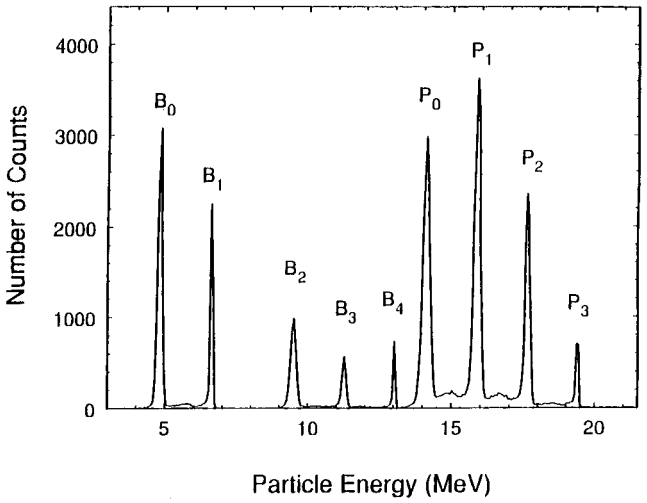

Figure 4. Energy spectrum of pulses from surface-barrier detector. DR of H_3^+ (6.5 MeV/nucleon) with perforated barrier inserted. P_3, all three H atoms pass through holes; P_2, two H atoms pass through holes and one passes through the solid portion; P_1, one atom passes through hole, two pass through solid; P_0, all three pass through the solid. The peaks labeled B are background peaks from breakup on collision with residual gas, e.g., B_0 and B_1 are H atoms which have passed through solid and hole, respectively, giving a measure of the foil transparency.

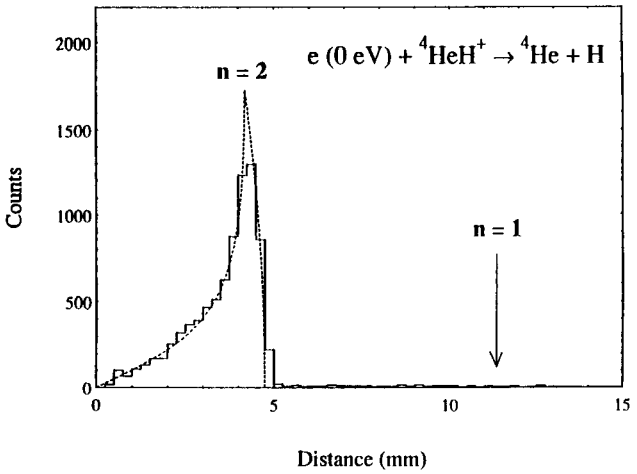

Figure 5. Position spectrum of the fragments from DR of HeH^+ using a position-sensitive microchannel plate detector. The separation measures the recoil kinetic energy which depends on the internal excitation states of the fragment atoms. In this case, zero collision energy, the exit channel yields exclusively H($n = 2$) atoms.

TABLE 1: Product Fractions in Dissociative Recombination of Triatomic Di-Hydrides

		fragment fraction	ΔE (eV)	ref
$H_3^+ + e$	$\rightarrow H_2 + H$	0.22	9.2	(5)
	$\rightarrow H + H + H$	0.78	4.7	
$H_2D^+ + e$	$\rightarrow DH + H$	0.2	9.2	(6)
	$\rightarrow H_2 + D$	0.1	9.2	
	$\rightarrow H + H + D$	0.7	4.7	
$CH_2^+ + e$	$\rightarrow CH + H$	0.25	5.8	(8)
	$\rightarrow H_2 + C$	0.12	6.8	
	$\rightarrow C + H + H$	0.63	2.3	
$NH_2^+ + e$	$\rightarrow NH + H$	–	7.5	(9)
	$\rightarrow H_2 + N$	–	8.2	
	$\rightarrow N + H + H$	0.66	3.7	
$OH_2^+ + e$	$\rightarrow OH + H$	0.19	7.4	(10)
	$\rightarrow H_2 + O$	0.08	7.6	
	$\rightarrow O + H + H$	0.73	3.0	–

4. Internal Excitation States of Recoiling Atoms from DR of Diatomic Molecules

As an example, take the case of one of the simplest molecular ions HeH^+ at "zero" collision energy:

$$HeH^+ + e \rightarrow He(1s^2) + H(1s) + 11.75\ eV \qquad (4a)$$

and

$$\rightarrow He(1s^2) + H(n{=}2) + 1.55\ eV \qquad (4b)$$

i.e., 11.75 and 1.55 eV kinetic energy release (KER), respectively, to the fragments. The KER can be determined by measuring the separation of the fragments after traversing the ~6-m distance from the DR region to a detector (see next section). The detector, in this case, is a microchannel plate, followed by a fluorescent screen and a CCD camera. A result is pictured in Figure 5. The shape is dictated by the dynamics, and is a two-dimensional projection of an isotropic distribution in the center-of-mass system. The maximum separation distance occurs for recoil perpendicular to the center-of-mass velocity in the lab system. The result in this case (approximately zero relative collision energy) is that all of the reaction results in formation of H atoms in the $n = 2$ state with virtually no H in the 1s ground state. As the relative energy is increased, there is shift to higher n values. Studies of the DR of $^4HeH^+$ and $^3HeH^+$ were carried out at both the Heidelberg and Stockholm rings.[7]

V. Dynamics of Three-body Breakup in Dissociative Recombination

As was mentioned above, triatomic species, especially dihydrides, show a large propensity for breaking up into three atoms, rather than an atom and a diatomic molecule. A list of the di-hydrides that have been measured thus far is given in Table 1. It includes in addition H_3^+,[5] H_2D^+,[6] CH_2^+,[8] NH_2^+,[9] and H_2O^+.[10] The reason for this effect is not at all clear. Is it a one-step or a two-step process? What are the excitation states of the atoms formed? How is the kinetic energy divided among the fragments? What are the angular distributions of the fragments?

The candidate molecular ion, in this case, is H_2O^+.[11] Because the O atom is much heavier than the H atoms, the recoil energy is taken up almost exclusively by the H atoms. At zero collision energy, only two three-body exit channels are energetically possible:

$$H_2O^+ + e \rightarrow O(^3P) + H(1s) + H(1s) + 3.04\ eV \qquad (5a)$$

$$\rightarrow O(^1D) + H(1s) + H(1s) + 1.02\ eV \qquad (5b)$$

The imaging detector used in this experiment (Figure 6) consists of three stacked microchannel plates (MCP) that generate flashes on a fluorescent screen. The pulses are amplified by an image intensifier and projected into a CCD camera and a multichannel-photomultiplier tube. The former records the separation of the fragments, and the latter is used to report the difference in arrival time of the fragments. The distance from the recombination region center is 6.4 m and, with stored beam energy of 4.5 MeV, the maximum H-atom displacement at the detector is 22 mm for the O(^{3}P) channel and 13 mm for the O(^{1}D) channel.

The plane containing the three fragments can have any orientation in space. It is only when this plane is parallel to the detector plane (i.e., perpendicular to the ion-beam axis) that the

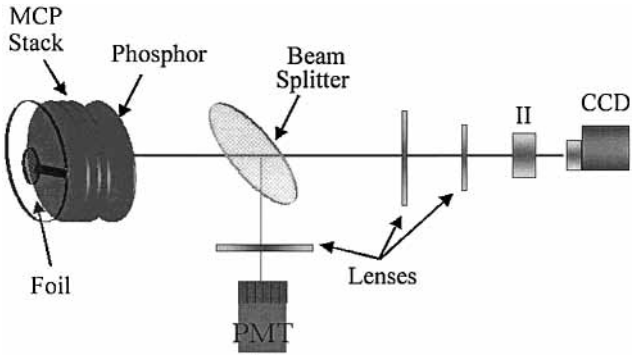

Figure 6. Detector system, microchannel plates, fluorescent screen, image intensifier (II), CCD camera, and multichannel-photomultiplier.

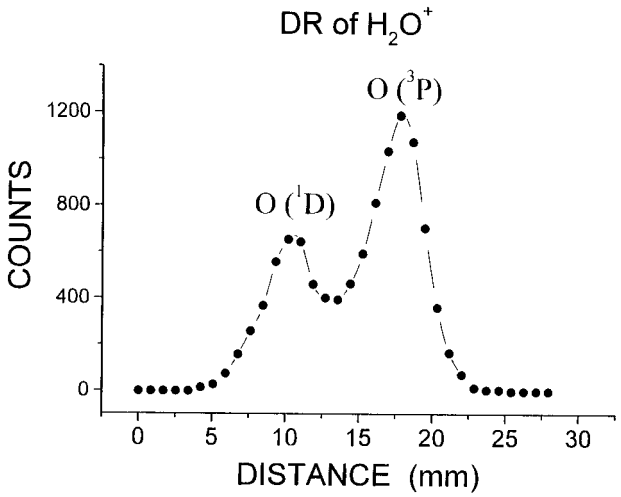

Figure 7. Measured distribution of total recoil distances (taken from the square root of the sum of the squares of the two O−H distances). The time window was <800 ps.

projected distances are a maximum and the true fragment velocities (and hence recoil energies) can be determined. Also, if the fragment plane is closely parallel to the detector plane, all three fragments should arrive at approximately the same time. Hence, we concentrate on the O−H distances in those triple events, which occur within a narrow time window (in this case <1 ns).

There remains one major problem. The H atoms and the O atoms give identical signals on a MCP detector. This was solved as follows. Because the O atom is so heavy, it is very little deflected from its original path. Therefore, in the center region of the MCP, we place an Al foil 2.5 μm thick and 5 mm in diameter (see Figure 7). If we operate the stored beam at 250 keV/amu, the 250-keV H atoms are stopped in the foil, but the 4-MeV O atoms pass through, emerge with ∼400 keV, and strike the MCP. Thus, we know that pulses arising in the region behind the foil must be due to O atoms and the remaining two pulses must come from H atoms whose positions with respect to the O atom can then be determined. From these data, we can measure the distances of the H atoms from the O atom and the angle between them. The first result is shown in Figure 7, where we plot the total recoil distance obtained from the square root of the sum of the squares of the $(O-H)_1$ plus $(O-H)_2$ distances. These points were obtained within a timing window of 0.8 ns. The upper portion is due to the O(^{3}P) channel and the lower one to O(^{1}D). From this spectrum, we derived the branching ratio O(^{3}P):O(^{1}D) = 3.5 ± 0.5:1.

To obtain the distribution of the kinetic energy released between the two hydrogen atoms for the O(^{3}P) channel, we use

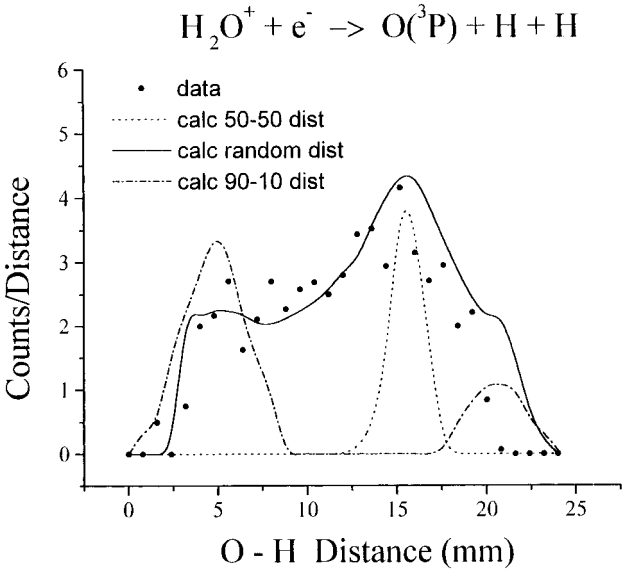

Figure 8. Distribution of recoil H atom distances in the O(^{3}P) channel divided by distance. Three models chosen for Monte Carlo analysis are chosen; - - - assumes 50:50 distribution between the two hydrogen atoms; − - − assumes a 90:10 division. The solid line is obtained using a random distribution.

those events whose total recoil distance (RD) is measured to be greater than 20 mm (see Figure 8). The selection of the uppermost edge is to limit consideration to events most parallel to the detector plane. For each H atom in a given H_2O molecular DR, we separately measure its recoil distance and plot the number of events at that distance divided by the distance, versus distance. This is a particularly convenient formulation for comparison with Monte Carlo calculations using different models. The data are plotted in Figure 8 for the O(^{3}P) case. Also shown are the results for three models. The narrow calculated peak assumes that the two hydrogen atoms share the total KER exactly (50−50 distribution). For a nonequal but sharply defined energy distribution (i.e., 90−10), we obtain the bimodal distributions shown. However, the best fit to the data is given by a random distribution of energies.

This lack of structure indicates the lack of a well-defined intermediate state, i.e., the existence of an intermediate excited state of OH. The vibrational distribution in a postulated OH* would surely smear any sharp binary distribution, but it is unlikely to completely eliminate it.

The distribution of angles between the two departing H atoms is plotted in Figure 9 for both the O(^{3}P) and the O(^{1}D) channels. Here again to ensure best fragment plane orientation, we use only the data from an upper slice of the measured recoil distances (Figure 8). For the O(^{3}P) case, we use RD ≥ 20 mm and for the O(^{1}D) case, we use 10 < RD < 14 mm. The line drawn for the O(^{2}P) is a two-point smooth and, for the O(^{1}D), we use a Lorenzian fit. However, both curves are just meant to "guide the eye."

The H−O−H bond angle in the ground states of both H_2O and H_2O^+ is ∼110°. In the case of O(^{3}P), there is no hint of preference in this angular region. The maximum is close to 0°, strongly indicating rearrangement prior to dissociation. A possibly relevant observation, in regard to the peaking at low angle, is that in the two-body DR channels, i.e., OH + H and O + H_2, the ratio (OH + H)/(O + H_2) is only a factor of 2, i.e., as though statistically distributed even though the O + H_2 channel would require considerable rearrangement to bring the two H atoms into close contact. (Note also in Table 1 that this

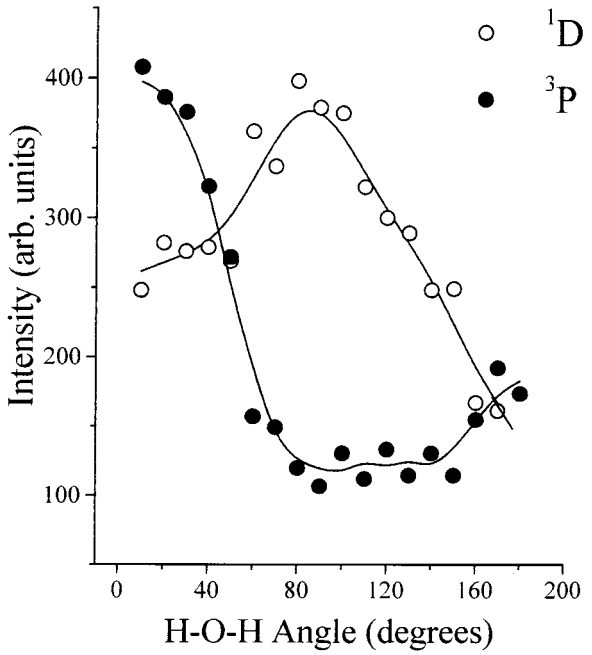

Figure 9. Angular distribution of the H atoms departing from H−O−H. For the O(^{3}P) channel, ●, the data used is from recoil distances >20 mm (Figure 2). The line is a two point smoothing to "guide the eye." For the O(^{1}D) channel, O, the data used is from recoil distances region 10−14 mm. The line is a Lorenzian fit to "guide the eye."

factor of ∼2 is also obtained in the H_2D^+ and the CH_2^+ cases. Although there has been no direct theoretical treatment of three-body DR dynamics, several publications may have a bearing on our observations. For example, Dixon and co-workers[12] did trajectory calculations on photodissociation of H_2O and showed that, along excited surfaces, there was considerable three-body decay and angular smearing. Child,[13] has speculated that dissociation proceeds via Rydberg states associated with the second excited superbent state B_2B2 of H_2O^+.[14] We note that at least one Rydberg state, ($\tilde{A}\ ^2A_1$) $3pb_2\ ^1B_2$, has been shown to be linear[1,12] and may be associated with the rise near 180°.

The net result of the present study is to give a detailed picture of the dynamics of three-body breakup in the DR of H_2O^+. The theoretical treatment of these observations has yet to be approached.

The "richness" of the physics involved can be further comprehended from some initial results of a recent study of the DR of NH_2^+ [15] using the same experimental setup. Here again two three-body exit channels are possible:

$$NH_2^+ + e \rightarrow N(^4S) + H + H + 3.67\ eV$$

$$\rightarrow N(^2D) + H + H + 1.29\ eV$$

The energetics are similar, yet a plot of total recoil distance as in Figure 8, we observe what appears to be a mirror image, i.e., the N(^{2}D) channel is dominant!

The state of DR theory has been highly developed for the treatment of diatomic systems. However, the treatment for even simple three-body systems is reminiscent of the phenomenological approaches used in the early days in other branches of chemical dynamics, a phenomenology which the contributions of Aron Kupperman have done much to clarify and quantify.

This research was sponsored by the U.S. Department of Energy, Office of Basic Energy Sciences, Division of Chemical Sciences under Contract No. DE-AC05-00OR22725 with UT-Battelle, LLC.

References and Notes

(1) Bates, D. R.; Massey, H. S. W. *Proc. Royal Soc.* **1947**, *A192*, 1.
(2) Mitchell, J. B. A. *Phys. Rep.* **1990**, *186*, 215.
(3) Datz, S.; Larsson, M. *Phys. Scr.* **1992**, *46*, 343.
(4) Larsson, M. *Annu. Rev. Phys. Chem.* **1997**, *48*, 151; Larsson, M. In *Adv. Gen. Phys. Chem. 10*: Photoionization and Photodetachment; Ng, C. Y., Ed.; World Scientific: Singapore, 2000; p 693.
(5) Datz, S.; Sundström, G.; Biedermann, C. H.; Broström, L.; Danared, H.; Mannervik, S.; Mowat, J. R.; Larsson, M. *Phys. Rev. Lett.* **1995**, *74*, 896.
(6) Datz, S.; Larsson, M.; Sundström, G.; Zengin, V.; Danared, H.; Kälberg; Ugglas, M. af. *Phys. Rev. A* **1995**, *52*, 1.
(7) Semaniak, J.; Rosén, S.; Sundström, G.; Datz, S.; Danared, H.; Larsson, M.; van der Zande, W. J.; Amitay, Z.; Hechtfischer, U.; Greiser, M.; Repnow, R.; Schwalm, D.; Wester, R.; Wolf, A.; Zajfman, D. *Phys. Rev. A* **1995**, *52*, R4320.
(8) Larson, Å.; Le Padellac, A.; Semaniak, J.; Stömholm, C.; Larsson, M.; Rosén, S.; Peverall, R.; Danared, H.; Djuric, N.; Dunn, G. H.; Datz, S. *Astrophys. J.* **1998**, *505*, 459.
(9) Vikor, L.; Al-Kalili, A.; Danared, H.; Djuric, N.; Dunn, G. H.; Larsson, M.; Le Padellac, A.; Rosén; Ugglas, M. af *Astron. Astrophys.* **1999**, *344*, 1027.
(10) Vejby-Christensen, L.; Andersen, L. H.; Heber, O.; Kella, D.; Pedersen, H. B.; Schmidt, H. T.; Zajfman, D. *Astrophys. J.* **1997**, *483*, 531; see also ref 12.
(11) Datz, S.; Thomas, R.; Rosén, S.; Larsson, M.; Derkatch, A.; Hellberg, F.; van der Zande, W. *Phys. Rev. Lett.*, submitted.
(12) Dixon, R. N.; Hwang, D. W.; Yang, X. F.; Harich, S.; Lin, J. J.; Yang, X. *Science* **1999**, *285*, 1249.
(13) Child, M. S. In "General Discussion," *Faraday Disc*. **2000**, *115*, 303.
(14) Pratt, S. T.; Dehmer, J. L.; Dehmer, P. M. *Chem. Phys. Lett.* **1992**, *196*, 469.
(15) Thomas, R. et al. In preparation.